Quaternary Science Reviews 295 (2022) 107766

Contents lists available at ScienceDirect

Quaternary Science Reviews

journal homepage: www.elsevier.com/locate/quascirev

Response of East Asian summer monsoon climate to North Atlantic meltwater during the Younger Dryas

Jie Wu [a, b], Zhengguo Shi [a, c, d, e, *], Yongheng Yang [b, f]

[a] State Key Laboratory of Loess and Quaternary Geology, Institute of Earth Environment, Chinese Academy of Sciences, Xi'an, 710061, China
[b] University of Chinese Academy of Sciences, Beijing, 100049, China
[c] Center for Excellence in Quaternary Science and Global Change, Chinese Academy of Sciences, Xi'an, 710061, China
[d] Institute of Global Environmental Change, Xi'an Jiaotong University, Xi'an, 710049, China
[e] Open Studio for Oceanic-Continental Climate and Environment Changes, Pilot National Laboratory for Marine Science and Technology, Qingdao, 266061, China
[f] Northwest Institute of Eco-Environment and Resources, Chinese Academy of Sciences, Lanzhou, 730000, China

ARTICLE INFO

Article history:
Received 31 March 2022
Received in revised form
20 August 2022
Accepted 9 September 2022
Available online 22 September 2022

Handling Editor: Qiuzhen Yin

Keywords:
Younger Dryas
Meltwater flux
East Asian summer monsoon
Westerlies
Paleoclimatology

ABSTRACT

The Younger Dryas (YD) event, recognized as one of the most typical abrupt climate changes on the millennial time scale, results in striking cooling in most regions of the North Atlantic. The most acceptable hypothesis believes that this event is related to a large volume of meltwater fluxes injected into the North Atlantic. In remote Asia, various paleoclimate reconstructions have revealed that the East Asian summer monsoon (EASM) is significantly depressed during the cold YD episode. However, the effect of North Atlantic meltwater-induced cooling on the whole downstream Eurasian regions and its potential dynamics remains been not fully explored till now. In this study, the responses of Asian climate characteristics during the YD episode, especially the EASM, are evaluated based on modeling data from the Simulation of the Transient Climate of the Last 21,000 years (TraCE 21ka). The results show that the cooling signal during the YD, which is mainly caused by meltwater flux, spreads from the North Atlantic to the whole Eurasia. In agreement with the paleoclimatic proxies, the simulated EASM is obviously weakened. The summer precipitation is also suppressed over East, South, and Central Asia. Dynamically, the North Atlantic cooling produces an eastward propagated wave train across the mid-latitude Eurasia, which facilitates weaker EASM circulation. The weakened land-sea thermal contrast over East Asia also contributes to the monsoon decrease during YD cooling.

1. Introduction

The Younger Dryas (YD) event, which happens about 12,900–11,700 years BP (Rasmussen et al., 2006), is recognized as a typical abrupt climate shift during the transition from the Last Glacial to the Holocene. As one of the climate events on the millennial-scale cycle, YD has been widely investigated and attracted more attention (Alley et al., 1993; Carlson, 2013; Grafenstein et al., 1999; Johnsen et al., 1992; McManus et al., 2004). In this event, the most striking feature is rapid and abrupt cooling over the North Atlantic Ocean, even extending to most regions of the Northern Hemisphere (NH) with different amplitudes, which exhibits an obvious geographic pattern (Broecker et al., 1988; Carlson, 2013). The YD event is originally identified in the pollen records in Northern Europe, and thereafter it has been recognized in numerous proxy reconstructions, such as the Greenland ice cores, marine and lake sediments, and the loess paleosol-records (An et al., 1993; Dansgaard et al., 1989; Keigwin and Jones, 1990; Kudrass et al., 1991; Zhou et al., 1999).

Several hypotheses have been proposed for the cause and mechanism of the YD and the most acceptable explanation refers to a collapse of the Atlantic Meridional Oscillation Circulation (AMOC) as a result of meltwater discharge. Generally, a large amount of glacial meltwater at the southern margin of the Laurentide Ice Sheet (LIS) reaching Lake Agassiz overflow to the Gulf of Mexico through the Mississippi River. During the YD, however, due to the retreat of the LIS, the diversion of meltwater discharge from the Mississippi River to the St. Lawrence River leads to increased

* Corresponding author. State Key Laboratory of Loess and Quaternary Geology, Institute of Earth Environment, Chinese Academy of Sciences, Xi'an, 710061, China.
E-mail address: shizg@ieecas.cn (Z. Shi).

https://doi.org/10.1016/j.quascirev.2022.107766
0277-3791/

freshwater in the North Atlantic Ocean (Broecker et al., 1989). A part of the meltwater from the LIS can reach the Arctic Ocean from Lake Agassiz through the Mackenzie drainage basin (Murton et al., 2010). Meltwater discharges decrease the density and salinity of the cold surface water and the rate of deep-water formation is reduced, which eventually slows down the AMOC (Broecker et al., 1988, 1989; Johnson and McClure, 1976; Rooth, 1982). The slowdown of the AMOC weakens the heat exchanges from low to high latitudes, resulting in a rapid reduction of the meridional northward heat transport and abrupt cooling of the North Atlantic extending to surrounding regions (Boyle and Keigwin, 1987; Broecker et al., 1985; McManus et al., 2004).

Besides the AMOC hypothesis, several other mechanisms have also been mentioned. Through an increase in precipitation together with iceberg influxes, an abrupt reduction in solar irradiance can cause a perturbation of the thermohaline circulation (THC), then may trigger the start of the YD (Renssen et al., 2000). Meanwhile, Wunsch et al. (2006) proposed that wind shifts associated with the ice sheet configuration can carry larger-scale ocean circulation signatures to the North Atlantic Ocean, triggering abrupt climate change like YD. Clement et al. (2001) indicated that tropical sea surface temperature (SST) changes related to orbital changes affect the freshwater export from the tropical Atlantic and THC. Recently, combined climate model simulations with a large number of proxy-based reconstructions, Renssen et al. (2015) pointed out that the causes of the YD event are more complex and might be a combination of the weakened AMOC, anomalous wind shift, and moderate radiative cooling. In addition, the origin of the YD event is also attributed to an extraterrestrial impact and associated high level of atmospheric dust (Firestone et al., 2007); however, this hypothesis has been highly debated by lots of evidence (Cheng et al., 2020; Pinter et al., 2011).

Paleoclimatic records have suggested that the YD event has profound impacts on global-scale climate changes. In the NH, there are cool and dry patterns with different amplitudes in most regions, such as the Greenland, Europe, North America (Alley, 2000; Brauer et al., 1999; deMenocal et al., 2000; Dorale et al., 2010; Genty et al., 2006; Shuman et al., 2005; Steffensen et al., 2008). However, a warming trend occurred in speleothem and pollen records in the Southern Hemisphere, implying the opposite signs between hemispheres (Hajdas et al., 2003; Moreno et al., 2009). Over the Asian continent, a large group of evidence suggests that it shows a relatively low temperature during the YD (Ding et al., 2017; Gasse and Van Campo, 1994; Morley et al., 2005; Nakagawa et al., 2003; Park et al., 2014). Sun et al. (2005) and Kubota et al. (2010) reveal that there has been a cooling of 0.5–1$^{\circ}C$ in the East China Sea. Based on the eolian and stalagmite records, a weakened Asian summer monsoon is consistently suggested during the YD episode (Beck et al., 2018; Sinha et al., 2005; Wang et al., 2001; Yuan et al., 2004; Zhou et al., 2014).

Climate model simulations have also been performed to explore the climatic responses to the freshwater hosting and changing AMOC intensity, which provides a reference for the climate dynamics during the YD event. Manabe and Stouffer (1988) firstly explored the responses of the freshwater discharge into the North Atlantic Ocean using a coupled ocean-atmosphere model and concluded that rapid cooling of climate occurred with meltwater impulse, which resembles the YD event. THC in the model weakens, causing a cool condition over the northern North Atlantic and the Greenland/Iceland/Norwegian Seas (Manabe and Stouffer, 1997). Vellinga and Wood (2002) illustrated a cooling in much of the NH while slightly warm in the Southern Hemisphere after the collapse of THC in their model. Correspondingly, precipitation is reduced in most regions of the NH. Significant cooling up to 2$^{\circ}C$ over Asia and a southward shift of the Intertropical Convergence Zone (ITCZ) over the Atlantic and eastern Pacific (Dong and Sutton, 2002; Timmermann et al., 2007; Zhang and Delworth, 2005). Sun et al. (2012) investigated the influences of the AMOC on the East Asian monsoon in water-hosting experiments and found a strengthening winter monsoon and a reduced summer monsoon with a slow-down AMOC. Recently, Yu et al. (2018) compared the variations of the East Asian monsoon in perturbed freshwater-hosing experiments with different intensities and proposed that northerly wind anomalies exist in East Asia in response to strong AMOC weakening.

In this paper, we mainly explore the evolution of the Asian climate during the YD, especially the Asian summer monsoon, using the transient climate simulations since the 21,000 years (TraCE 21ka). The responses of East Asian and Indian summer monsoon during the YD event and their attributions are evaluated. In section 2, an introduction of the modeling data is given and the whole YD period is selected. The results are presented in section 3, including the climate responses in Asia under different forcing. The discussion and conclusion are finally listed in section 4 and section 5, respectively.

2. Data and methods

The TraCE 21ka experiments are performed by the Community Climate System Model version 3 (CCSM3) from the National Center for Atmospheric Research (NCAR), which is a fully coupled atmosphere-ocean-sea ice-land surface climate model without flux adjustment (Collins et al., 2006). The experiment set contains a full forcing simulation (TraCE-FULL) from 22 ka BP to 1990 CE as well as four single-forcing sensitivity simulations (TraCE-ORB, TraCE-GHG, TraCE-ICE, TraCE-MWF) of varying lengths, which are driven by the realistic climatic forcings of orbitally-driven insolation changes, transient greenhouse gas concentrations, continental ice sheets, and meltwater fluxes.

In transient experiments, the concentrations of greenhouse gases (CO_2, CH_4, and N_2O) are adopted from Joos and Spahni, 2008, and the changes in orbital insolation are derived from Berger (1978). The ice sheet configurations including the heights and extents are mainly modified approximately once per 500 years according to the ICE-5G reconstructions (Peltier, 2004), aiming to obtain more realistic coastlines in the model. During the YD period, the meltwater fluxes are mainly discharged into the St. Lawrence River and Mackenzie River, and the greenhouse gas concentrations have subtle changes of less than 10 ppmv. All these simulations are conducted at the T31_gx3 resolution (Yeager et al., 2005) with an enabled dynamic global vegetation module. More detailed information about the model setup can be found in He (2011) and He et al. (2013). This modeling dataset has been widely applied in paleoclimatic studies and proved to give reasonable performance over Asia (Liu et al., 2012; Shi and Yan, 2019; Wen et al., 2016).

In order to evaluate the response of the Asian climate, we first examined the evolution of annual surface temperature in the NH and selected the YD stage (Fig. 1). It is clear that TraCE-FULL simulation can capture the main characteristics of the climate fluctuations from the Last Glacial Maximum to the Holocene, in good agreement with the Greenland ice cores. The time series reproduces the abrupt cooling and recovery, clearly indicating the start and the end of the YD event. The AMOC strength also exhibits synchronous changes with the simulated surface temperature variation over the NH, indicating the drastic weakening and recovery during the YD period. Based on the time of temperature and summer precipitation variation, the pre-YD and peak YD are denoted as 13.2–12.9 ka BP and 12.3–12.0 ka BP, respectively, and their differences (denoted as the mean values of the peak YD minus the pre-YD) are calculated as the climatic responses. In this study,

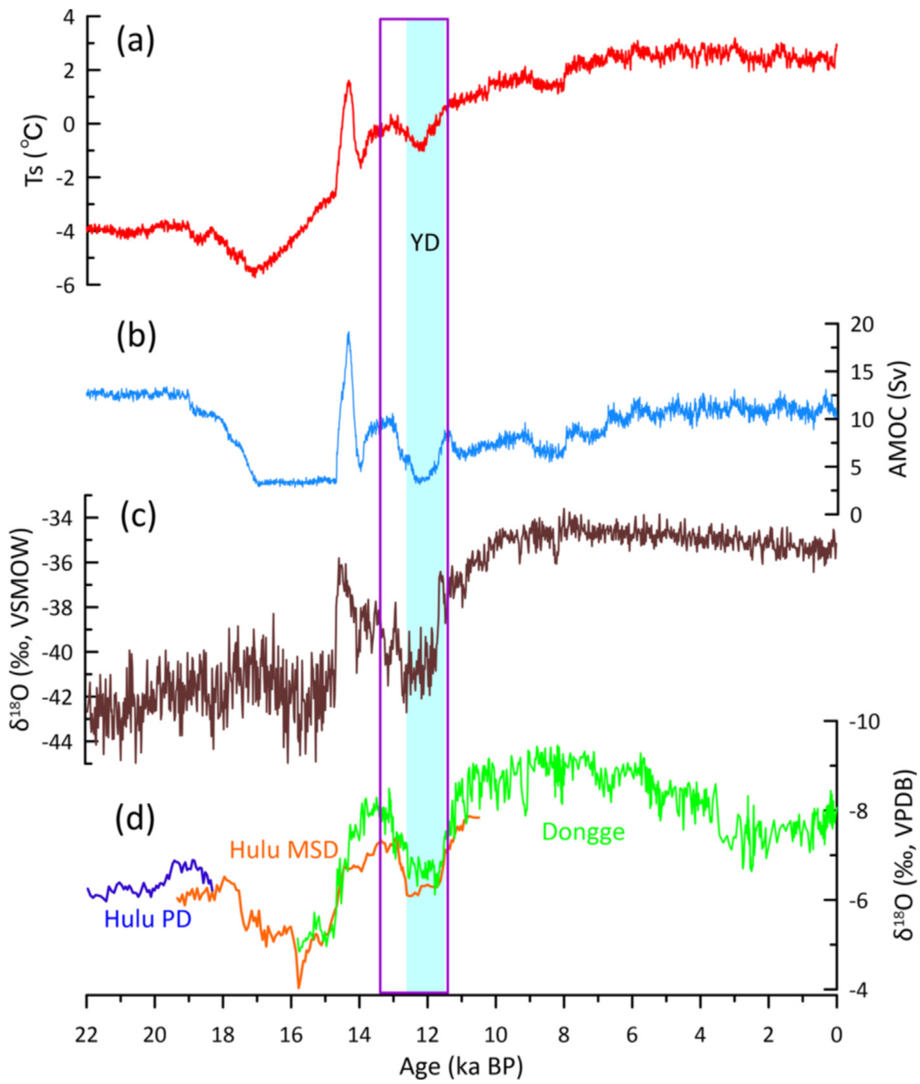

Fig. 1. Evolution of simulated and reconstructed climate indices. (a) Northern Hemisphere surface temperature based on TraCE 21ka full-forcing simulation, (b) The simulated AMOC strength (defined by the maximum of the Atlantic overturning stream function below 500 m depth), (c) $\delta^{18}O$ from the North Greenland Ice Core Project (Rasmussen et al., 2006), (d) the East Asian summer monsoon records from the Dongge and Hulu cave stalagmites (Wang et al., 2001; Yuan et al., 2004). The light blue bar represents the Younger Dryas event. The purple box shows the time stage which is selected in Fig. 3. (For interpretation of the references to colour in this figure legend, the reader is referred to the Web version of this article.)

the boreal summer months include June, July, and August (JJA) while the winter is denoted as December, January, and February (DJF).

Several typical sub-regions in Asia (10–70° N, 60–130° E) are defined (Fig. 2), including Tibetan Plateau (TP, 25–40° N, 70–105° E), East Asian monsoon (EA, 25–35° N, 105–130° E), South Asian monsoon (SA, 10–25° N, 65–85° E), and Central Asian arid regions (CA, 40–50° N, 60–95° E), respectively. As the main source of the meltwater discharge, the North Atlantic (NA, 50–70° N, 80°W-20° E) is also included.

3. Results

The time series of anomalies of the surface temperature and precipitation over typical sub-regions in the TraCE-FULL simulation are shown in Fig. 3. Surface temperature and precipitation all show synchronous variations during the YD but with different amplitudes in each sub-region. The cooling begins at about 13.0 ka BP, reaches the peak at 12.2 ka BP and recovers to normal. The strongest cooling over NA nearly reaches up to 3.5 °C (Fig. 3a), while it is similar in Asia and TP with a smaller amplitude of 0.6 °C (Fig. 3c,e). The variation of summer precipitation anomalies generally resembles that of surface temperature during the YD period, and less rainfall changes occur in EA and CA during the YD period than that in SA (Fig. 3b,f). In SA, it is clear that the precipitation decreases from 13.2 ka BP to 12.3ka BP, with nearly 2 mm day^{-1} (Fig. 3d).

The spatial differences between the peak YD and pre-YD in annual surface temperature and summer precipitation over Asia in the TraCE-FULL simulation are shown (Fig. 4). During the YD event, a significant cooling is simulated in the North Atlantic Ocean. The mid-to-high latitude North Atlantic surface temperature shows strong cooling with a maximum of about 10 °C. This cooling signal in North Atlantic spreads downstream throughout Europe and eventually extends to most of Asia. A cooling center over Greenland and a warming center over the Barents Sea present a surface temperature dipole and this dipole pattern is also described in several freshwater perturbation experiments, which might be

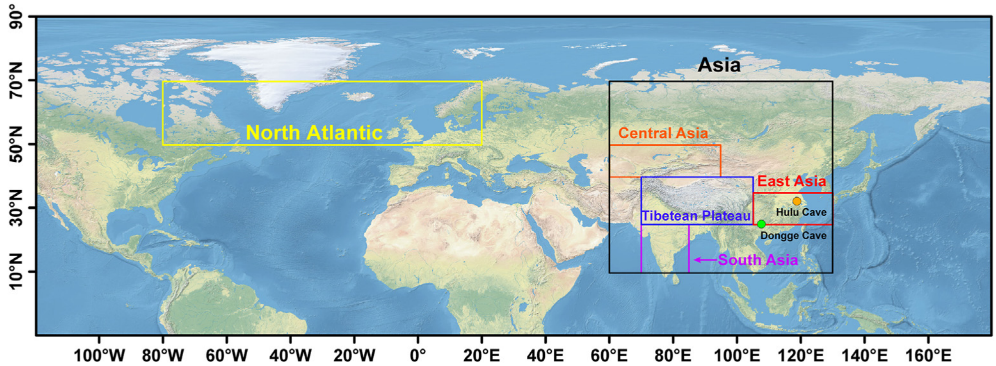

Fig. 2. Locations of the focused regions in this study. North Atlantic: 50–70° N,80°W-20° E; Asia: 10–70° N,60–130° E; Tibetan Plateau: 25–40° N,70–105° E; East Asia: 25–35° N,105–130° E; South Asia: 10–25° N,65–85° E; Central Asia: 40–50° N,60–95° E. The orange and green dots represent the locations of stalagmite records from Hulu Cave and Dongge Cave, respectively. (For interpretation of the references to colour in this figure legend, the reader is referred to the Web version of this article.)

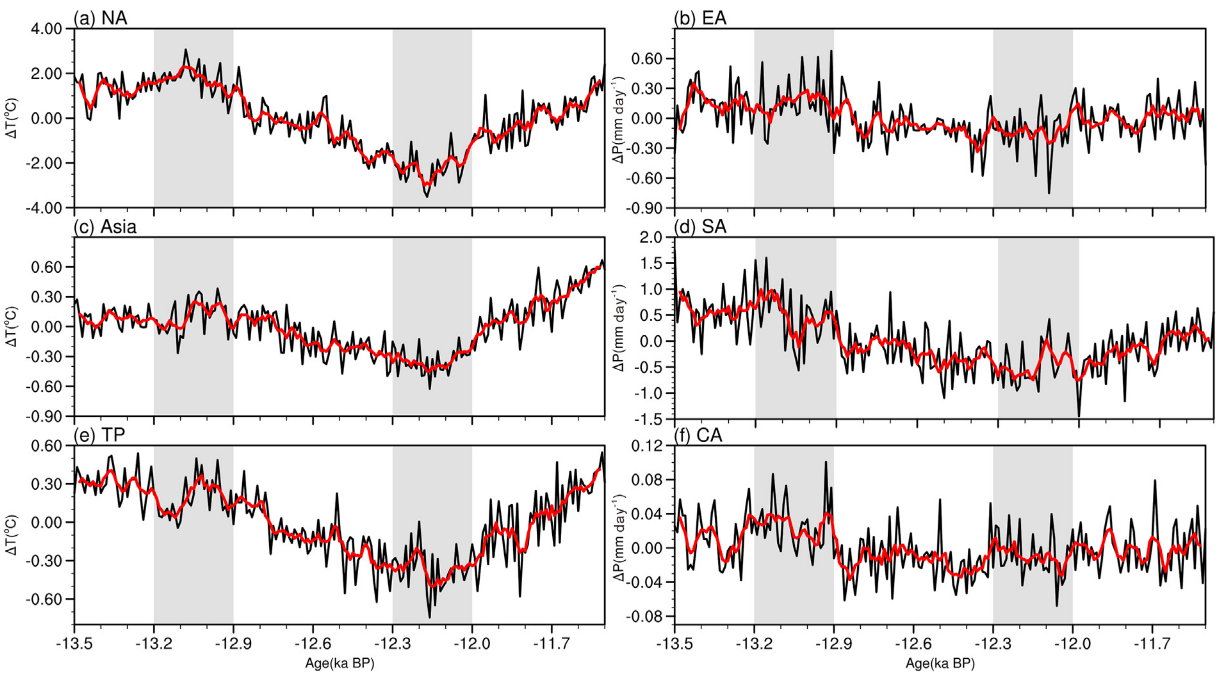

Fig. 3. Time series of anomalies of annual averaged surface temperature and summer precipitation rate over typical sub-regions during the YD (black line). a, c, e is for surface temperature of North Atlantic, Asia, and Tibetan Plateau, respectively, b, d, f is for summer precipitation rates of East Asia, South Asia, and Central Asia. The red solid lines represent the 50-year running mean. Grey shaded boxes show the periods of pre-YD (13.2–12.9 ka BP) and peak YD (12.3–12.0 ka BP). The reference period to calculate the anomalies is 13.5–11.5 ka BP. (For interpretation of the references to colour in this figure legend, the reader is referred to the Web version of this article.)

related to the location in which the freshwater flux is discharged (Dahl et al., 2005; Stouffer et al., 2006). The different amplitudes of cooling occur in Asia while an increasing temperature is simulated over the Indian subcontinent, similar to the results of Marzin et al. (2013). A cooling atmosphere results in less precipitation in the mid-latitude areas of the NH (Fig. 4b). The wind field exhibits strong northerly and northwesterly wind anomalies from Central Asia to the northern Indian Peninsula but easterly and southeasterly winds over the Arabian Sea, which indicates weakened Indian summer monsoon (ISM) and decreased precipitation in South Asia by 0.13–2.22 mm day^{-1}. Anomalous northeasterly winds dominate over EA, meaning that the EASM is also weakened (Fig. 4b). However, the precipitation is not consistently suppressed over East Asia and exhibits a tripole pattern instead. In addition, slightly decreased precipitation in Central Asia is detected but insignificant over most of the regions (Fig. 4b).

To evaluate the responses of temperature to individual forcing in the YD event, the spatial characteristics of annual and seasonal surface temperature are shown (Fig. 5). Basically, there show similar geographic distributions between the annual, summer, and winter changes, but with different amplitudes. In the TraCE-MWF experiment, there is widespread cooling throughout the North Atlantic to the Eurasian continent with the most significant over North Atlantic (Fig. 5a). In contrast, the Tibetan Plateau and South Asia, and the subtropical North Atlantic Ocean experience warming, which is similar to the TraCE-FULL results (Fig. 4a). The cooling becomes smaller in summer but larger in winter (Fig. 5b–c). In the TraCE-ICE experiment, decreased ice sheets lead to considerable annual warming over most of the NH regions and the warming has larger magnitudes over high latitudes than low latitudes (Fig. 5d). However, remarkable cooling occurs over North Atlantic Ocean. In summer, there shows more intensive warming in the whole NH

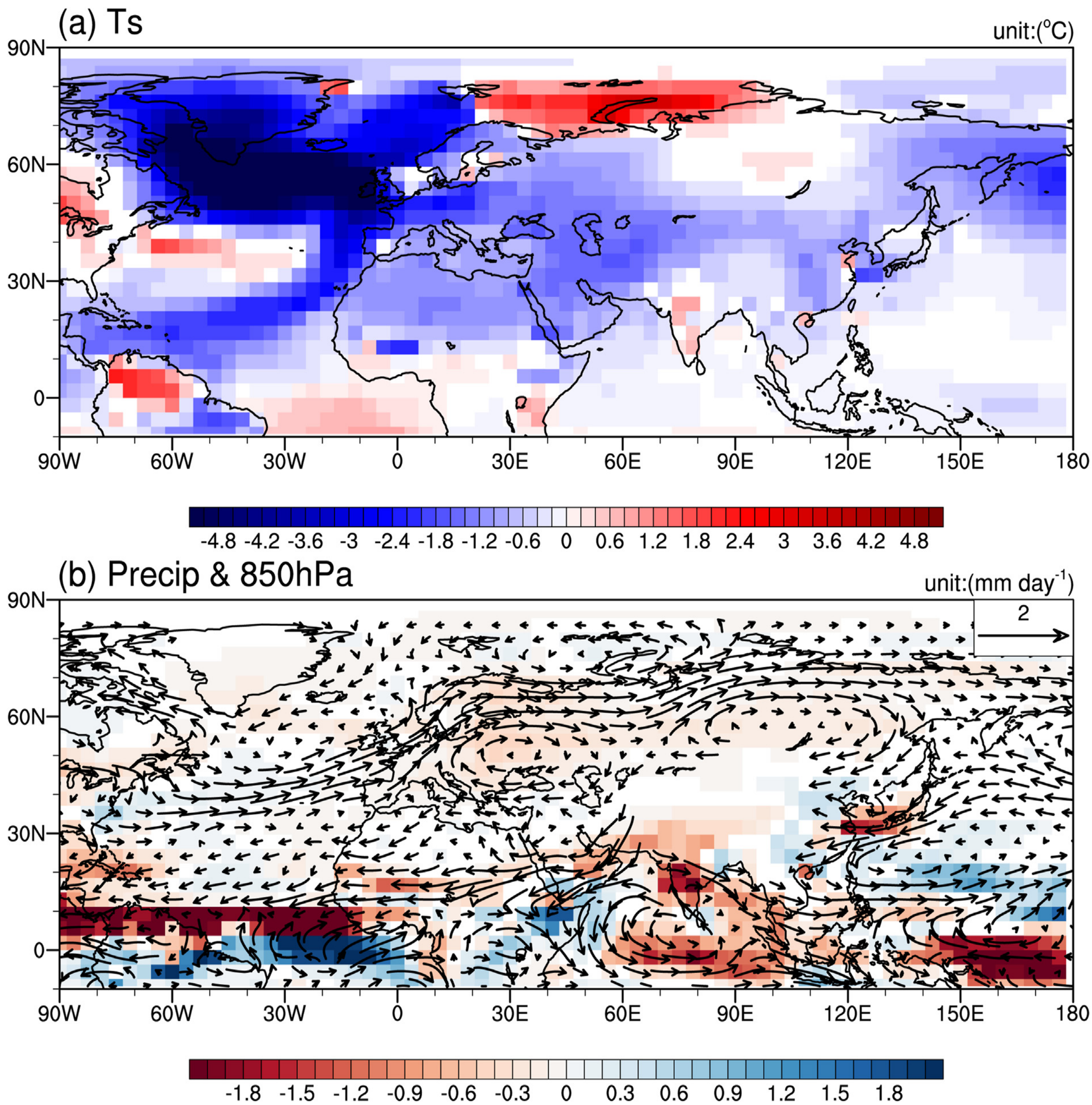

Fig. 4. Changes in (a) annual surface temperature (shaded), (b) summer precipitation rate (shaded), and 850 hPa wind (vectors) in the TraCE 21ka full-forcing simulation during the YD. Only differences that exceed the 95% significant level are plotted.

continent (Fig. 5e), but a larger cooling occurs across the North Atlantic, Europe, and North Africa in winter (Fig. 5f). Opposite to ice sheets, the greenhouse gas reduction induces anomalous cooling over the entire NH in the TraCE-GHG annually and seasonally (Fig. 5g, h, and 5i), which shows that greater cooling in high latitudes and moderate in low latitudes. From the TraCE-ORB, modest warming is detected in high-latitude Eurasia while a slight cooling is in low latitudes (Fig. 5j, k, and 5 l).

The spatial patterns of summer precipitation and 850 hPa summer wind for individual forcing are shown in Fig. 6, respectively. The meltwater forcing in the TraCE-MWF experiment produces significantly dry conditions in Asia, especially over South Asia and East Asia (Fig. 6a), which explains nearly the whole of entire changes during the YD event (Fig. 4b). The 850 hPa wind vectors show northerly wind anomalies over East Asia and anomalous northwesterly in South Asia (Fig. 6b), indicating weakened East Asian and Indian summer monsoon. Unlike the TraCE-MWF, the changes in summer precipitation are relatively small over Asia in the TraCE-ICE, TraCE-GHG, and TraCE-ORB (Fig. 6c, e, and 6g). In the TraCE-ICE, the precipitation significantly increases in northern East Asia but decreases in the southern regions, which is related to the wind variations (Fig. 6d). In the TraCE-GHG, the 850 hPa summer wind anomalies are stronger with anti-cyclonic circulation anomalies over subtropical western Pacific (Fig. 6f), however, the precipitation presents insignificant changes (Fig. 6e). In the TraCE-ORB, there show southerly wind anomalies in East Asia and anomalous northwesterly in South Asia (Fig. 6h).

Quantitative contributions of individual forcing to the total changes of Asian climate in some typical regions are then calculated (Fig. 7). Over NA, the annual and seasonal surface temperature in the TraCE-FULL all decreases, and the maximal cooling, up to 7.5 °C during the winter. Compared to the TraCE-FULL, the TraCE-MWF

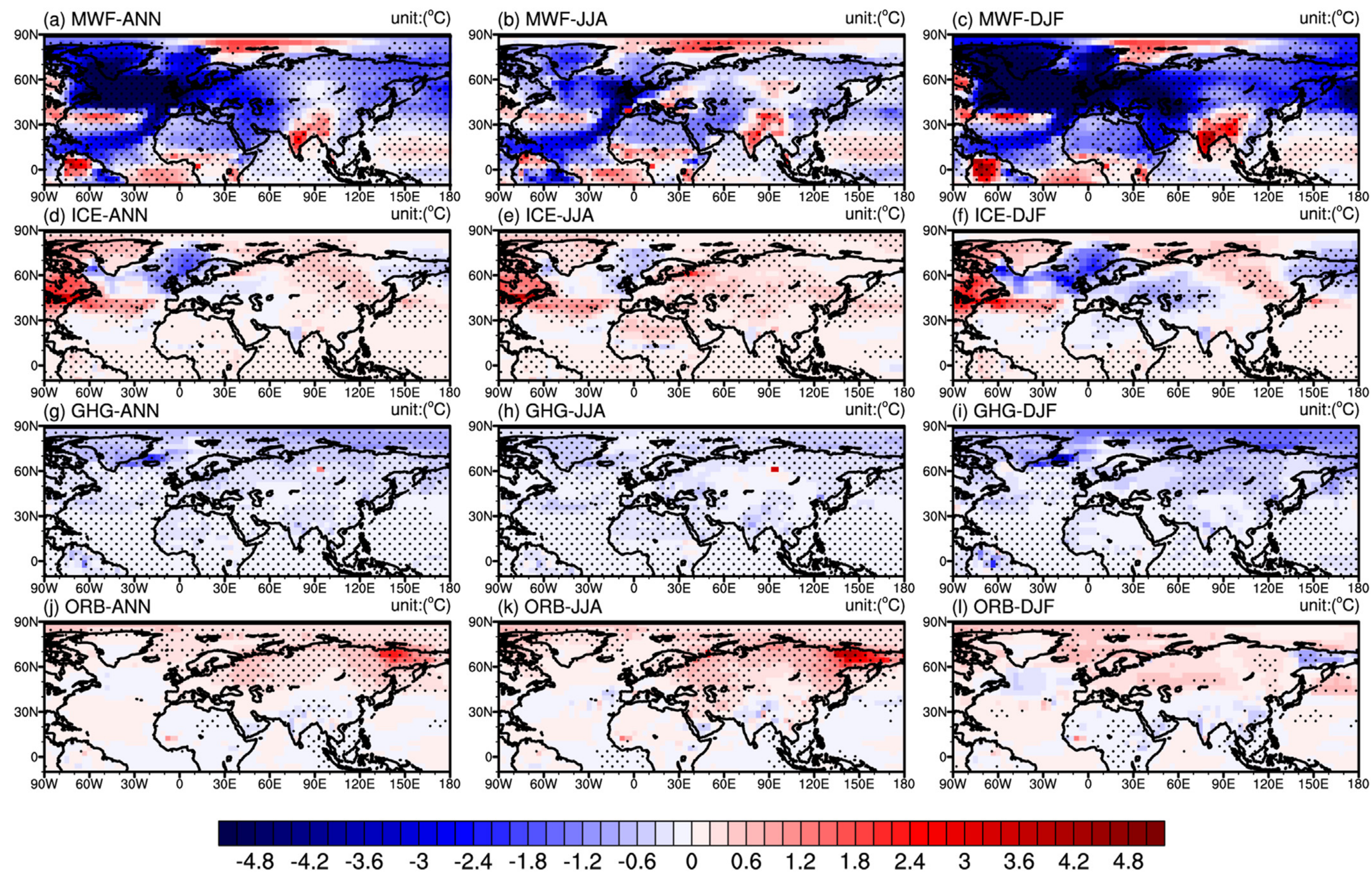

Fig. 5. Changes in surface temperature in the TraCE 21ka single-forcing simulation during the YD. (a–c) annual, summer, and winter temperature in the TraCE-MWF experiment, (d–f) similar with a-c, but for TraCE-ICE, (g–i) TraCE-GHG, and (j–l) TraCE-ORB, respectively. Dotted show the changes significant at the 95% confidence level.

temperature has similar but larger variations in NA, suggesting that the meltwater discharge exerts great influence on surface temperature during the YD. The single-forcing experiments with ice sheets, greenhouse gases, and orbital parameters produce subtle temperature changes compared with that with the meltwater flux (Fig. 7a). Over Asia, a moderate decrease is simulated in the TraCE-FULL, TraCE-MWF, and TraCE-GHG. In TP, a major decline in temperature happens during the winter but a slight decrease happens in summer in the TraCE-FULL simulation. However, opposite to the other two regions, anomalous warming, especially in winter, appears over TP in the TraCE-MWF (Fig. 7e). Over Asia and TP, the greenhouse gases also induce temperature declines, which contributes a part to the total cooling in YD (Fig. 7c,e). However, the warming is seen in the annual and summer mean in the TraCE-ICE, partly counterbalancing the meltwater-induced cooling. Obvious summer precipitation changes mainly occur over EA and SA (Fig. 7b,d) due to the weakened East Asian and Indian monsoon. Both the TraCE-FULL and TraCE-MWF show stronger negative anomalies during the YD. Winter rainfall is relatively small and insignificant in EA and SA except that the TraCE-FULL produces more precipitation over EA. Over CA, which is dominated by the westerlies, the changes in precipitation are concentrated in winter (Fig. 7f) and smaller precipitation is mainly observed in TraCE-FULL, TraCE-MWF, and TraCE-ICE. For annual and seasonal precipitation, the TraCE-MWF simulation has nearly the largest decreases, which indicates that meltwater flux is the most important external forcing that affects precipitation during the YD.

To further elucidate the mechanism of how North Atlantic meltwater affects the Asian climate during the YD, we focus on the responses in the TraCE-MWF simulation, and the distribution patterns of sea level pressure (SLP) in summer are given (Fig. 8). Combined with Fig. 5b, it can be seen that the whole Asia experiences cool conditions except for TP and SA, which shares similar characteristics with the TraCE-FULL (Fig. 4a). Negative SLP anomalies appear over the northwestern Pacific and slightly positive anomalies are over East Asia. Due to different heat capacities, the land-sea thermal contrast decreases, resulting in a weaker EASM circulation. An anomalous cyclonic circulation develops over the northwestern Pacific (Fig. 8), which is responsible for the anomalous northerly winds over EA (Fig. 6b). In the north of the equator, a cooling and less precipitation over the eastern tropical Pacific off the coast of Central America (not shown) while an enhancement of summer precipitation over the western tropical Pacific (Fig. 6a), which indicates a strengthened Walker Circulation, and leads to a weakened EASM and less rainfall (Yu et al., 2009). Strong cooling appears in the Arabian Peninsula and positive SLP anomalies are produced. Together with negative SLP anomalies over the southern Indian Ocean, they result in anomalous surface northerly winds over the Arabian Sea, weakening the cross-equatorial air stream and thus the ISM. Additionally, Zhang and Delworth (2005) suggested that the weakening and eastward shifts of the Walker Circulation over the south of the equator can induce weaker ISM and less rainfall by suppressing convective heating. Meanwhile, due to the weakened cross-equatorial air stream, less moisture transport to the SA may lead to fewer clouds and more shortwave radiation at the surface, which explains the warm conditions over SA and surrounding areas (Fig. 5b). In addition, a large cooling occurs over the subpolar and tropical North Atlantic, and anomalous warming is

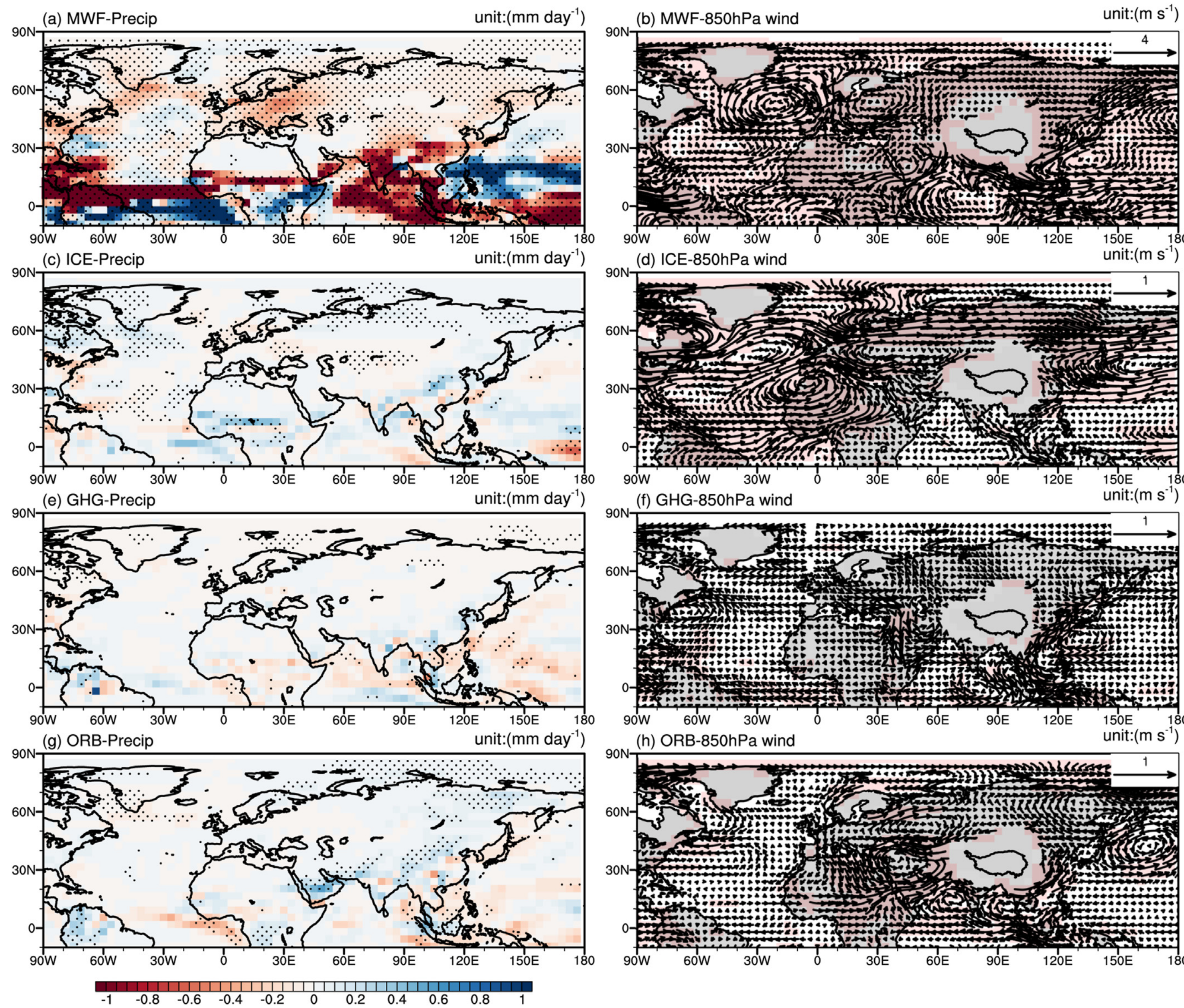

Fig. 6. Changes in summer precipitation rate (shaded) and 850 hPa wind (vectors) in the TraCE 21ka single-forcing simulation during the YD. (a, b) TraCE-MWF, (c, d) TraCE-ICE, (e, f) TraCE-GHG, and (g, h) TraCE-ORB. Dotted and red shaded mean the precipitation and wind differences significant at the 95% confidence level, respectively. (For interpretation of the references to colour in this figure legend, the reader is referred to the Web version of this article.)

mainly located in the subtropical ocean, indicating an anomalous negative-positive-negative tripole pattern of SST (Fig. 5b). Subsequently, a deepening of the Icelandic low and a strengthening of the Azores high share a similar structure of positive phases of the North Atlantic Oscillation (NAO).

The zonal mean deviations of geopotential height at 200 hPa in the TraCE-MWF are presented (Fig. 9). It is clear that a zonal wave-train pattern develops across the North Atlantic and Eurasia in the upper troposphere. An anomalous anticyclonic-cyclonic-anticyclonic circulation pattern eventually leads to the weakening high pressure over the Ural Mountain and the Okhotsk Sea (Fig. 9). These high-tropospheric circulation changes also contribute to the response of EASM. From a viewpoint of moisture transport, an anomalous negative moisture flux convergence is simulated over EA with northeastern moisture flux anomalies (Fig. 10b), combined with anomalous sinking motion as seen in 500 hPa vertical velocity (Fig. 10a). Most parts of the Indian Peninsula are dominated by the anomalous northwesterly winds and strong anomalous sinking motion (Figs. 6b and 10a), which is responsible for the lighter precipitation there. Over CA, there are positive vertical velocity anomalies (Fig. 10a), which suppress the rainfall. The winter atmospheric circulation has similar patterns to the summer (not shown), also accounting for the deficits in rainfall.

4. Discussion

The TraCE-21ka results reveal that the whole Asia broadly experiences extremely cool and dry conditions in main response to the meltwater discharge and subsequent strong cooling in North Atlantic, which is in general agreement with current proxies. For instance, Fukusawa (1999) analyzed the records of the varved layers from Lake Suigetsu and Lake Tougouike and suggested that a dry and cold climate occurred in inner Asia, reflecting a YD signature. By evaluating mean effective moisture paleoclimatic records from monsoonal Central Asia, Herzschuh (2006) found that "moderate dry" or "dry" conditions of the YD dominated in most of

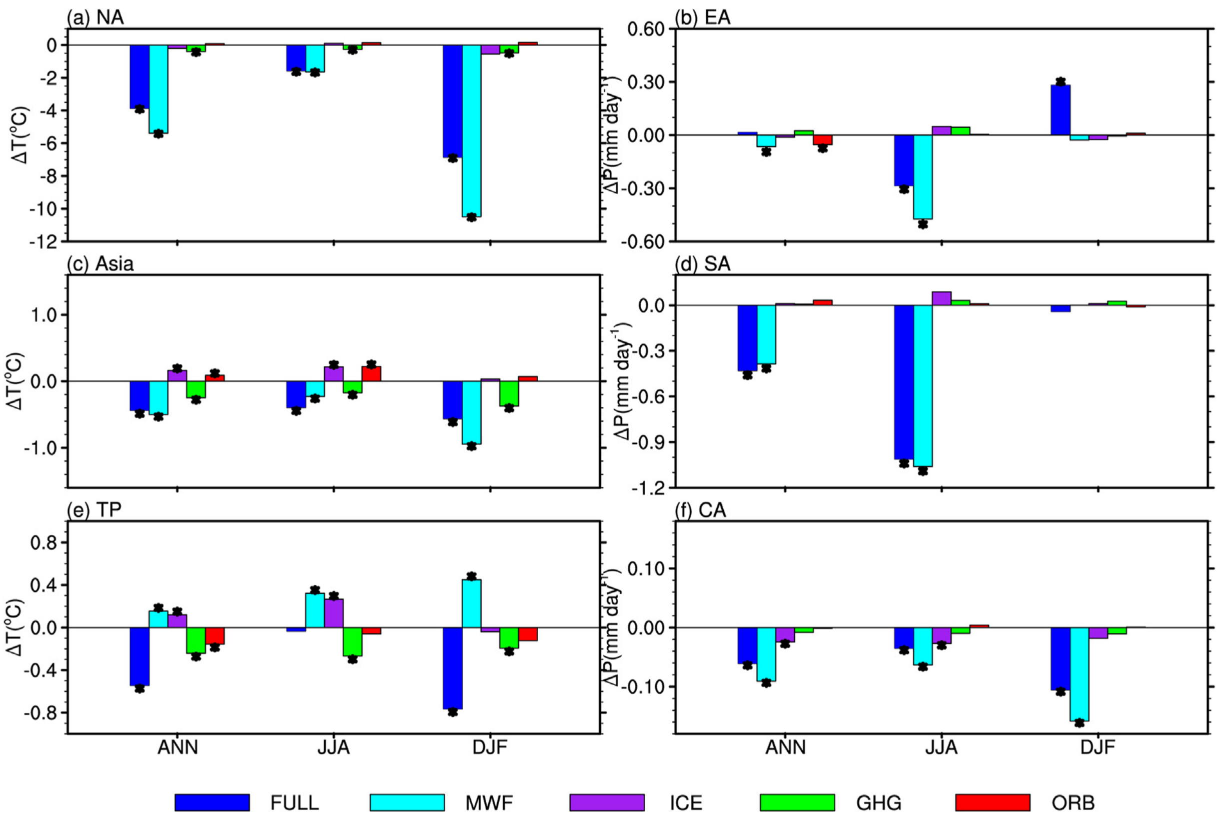

Fig. 7. Differences in surface temperature and precipitation rates over typical sub-regions in the TraCE 21ka full-forcing and single-forcing simulations during the YD. a, c, e is for surface temperature over North Atlantic, Asia, and Tibetan Plateau, respectively, b, d, f is for precipitation rates over East Asia, South Asia, and Central Asia. Asterisks represent differences exceeding the 95% significance level.

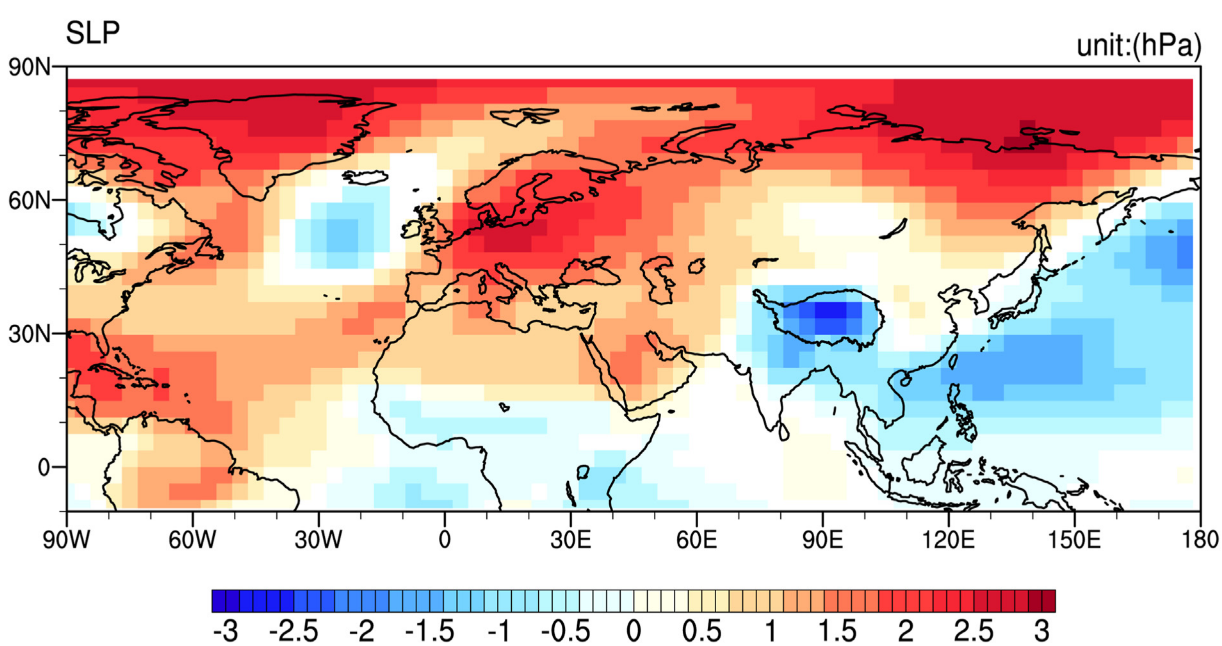

Fig. 8. Changes in sea level pressure in summer in the TraCE-MWF during the YD. Only differences that exceed the 95% significant level are plotted.

northeastern and eastern China. Such cool and dry climate during the YD episode is also found in pollen records, linking to the shifts in the elevation of vegetation zones and the changes of vegetation composition (Chen et al., 2020; Nakagawa et al., 2006; Takahara et al., 2010). Moreover, high-resolution speleothem in the East Asian monsoon region and pollen records from northern China have revealed that the EASM intensity becomes weaker (Chen et al., 2015; Dykoski et al., 2005; Liu et al., 2008; Ma et al., 2012). The

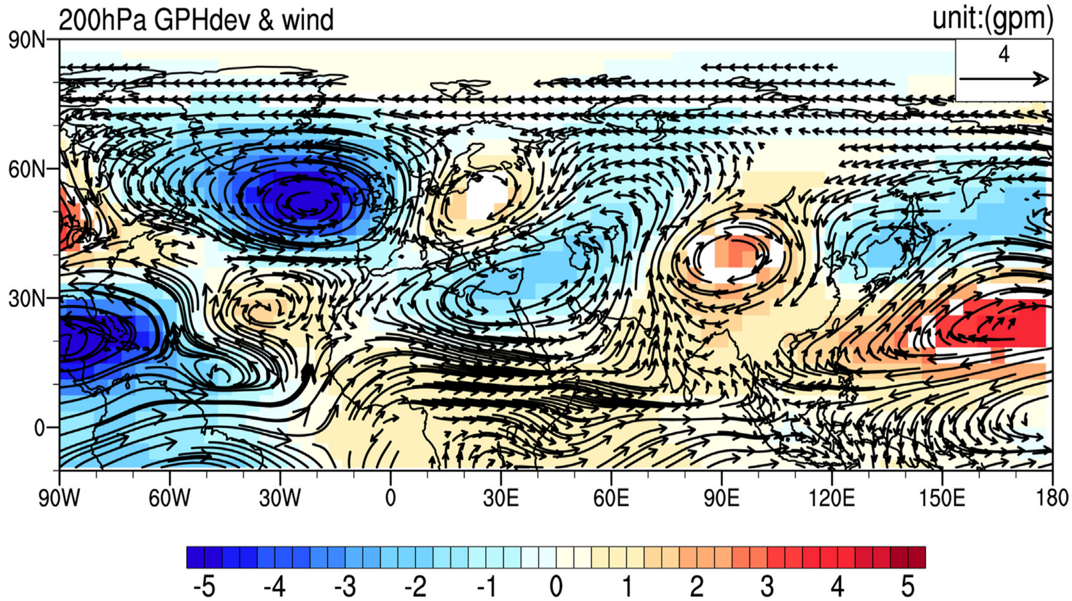

Fig. 9. Changes in zonal deviations of geopotential height (shaded) and winds vectors at 200 hPa in summer in the TraCE-MWF simulation during the YD. Only differences that exceed the 95% significant level are plotted.

proxy-based weakened East Asian monsoon intensity during YD is consistent with the simulated weakened summer circulation, even not very well with simulated precipitation variation over East Asia. Although the geological evidence for the ISM is not sufficient, previous studies indicated that the weakened ISM during the YD was coherent with the EASM, based on the marine sediments and stalagmite isotopes (Rashid et al., 2007; Shakun et al., 2007; Sinha et al., 2005).

Meltwater flux exerts a profound impact on the Asian climate during the YD, which is considered to trigger this event by slowing down the state of the AMOC. Alley (2007) believed that an AMOC weakening might be related to a number of centennial-to-millennial-scale cool events, including the Heinrich, Younger Dryas. Various climate model experiments also support the impacts of the AMOC intensity on global climate through the addition of freshwater discharge into the North Atlantic (Manabe and Stouffer, 1997; Okumura et al., 2009; Wu et al., 2008). Vellinga and Wood (2002) explored the climate response to a weakened AMOC and suggested that a cool condition spreads over large parts of the NH effectively by the atmospheric circulation, as well as a cooling up to 2 °C in Asia. By analyzing the multi-model ensemble data, Stouffer et al. (2006) found negative precipitation anomalies and cool surface air temperature in Asia, as a result of decreased AMOC caused by freshwater input. Our results indicate that the EASM circulation and ocean-land thermal contrast are both reduced under the meltwater flux forcing during the YD episode. Similar to our conclusion, some water-hosting perturbation experiments under the present-day conditions also found that the weakening of the AMOC produces northerly wind anomalies over East Asia in summer, suggesting the decreased EASM (Lu and Dong, 2008; Yu et al., 2009, 2018; Zhang and Delworth, 2005). These studies have revealed that the freshwater discharge can affect the EASM through tropical processes. For example, Yu et al. (2009) show strong cooling occurring over the North Atlantic and North American continent, and warming in the south Atlantic, which indicates a southward shift of the ITCZ, leads to weakened Hadley Circulation but strengthened Walker Circulation in the tropical Pacific, and thus induces weaker EASM. Zhang and Delworth (2005) also found that the northern Pacific exhibits a La Nina-like pattern with a stronger Walker Circulation with the weakened AMOC, as well as a southward displacement of the ITCZ. Yu et al. (2018) proposed that the northerly wind anomalies are caused by an anomalous westward SLP gradient between Eurasia and the northwestern Pacific, which is related to heat flux anomalies in the South China Sea and the Philippian Sea.

Our analysis confirmed that the meltwater discharge produces lower surface temperature in the North Atlantic, which exhibits a tripole SST anomaly pattern, indicating a typical structure of a positive phase of NAO. And this cooling pattern can remotely affect the EASM by the modulation of the upper-tropospheric westerlies; this mechanism also gains support from modern climatic research. Previous studies have pointed out that a North Atlantic tripole SST anomaly pattern associated with NAO phase anomalies can excite the teleconnection from the North Atlantic to Eurasia connecting by an eastward propagated wave train, affecting the East Asian subtropical front and further EASM (Wu et al., 2009; Zuo et al., 2013). Zheng et al. (2016) also concluded that the NAO signal can imprint on contemporaneous SST pattern and further modulate the EASM, which becomes an important predictor for EASM. Zuo et al. (2013) found that the meridional location of the tripolar SST pattern is sensitive to the north-south movement of the NAO center, which has a potential impact on EASM. Based on model simulations, Sundaram et al. (2012) indicated that the signals of summer NAO can affect the EASM through the stationary waves excited at the Asian Jet entrance during the Marine Isotope Stage (MIS) 13.

Our results have captured the characteristics of the Asian climate response to North Atlantic meltwater during YD and emphasized the low and high latitude dynamics of monsoon circulation. However, it should be noticed that uncertainty still exists in model sensitivity and interpretation of the proxy especially when the YD-like millennial-scale abrupt climate events are focused. Our analysis failed to give an exact spatial agreement between TraCE-FULL precipitation and East Asian stalagmite isotopes. On the one hand, different inter-model responses during the YD cannot be ignored. Renssen (2020) pointed out that large uncertainties are mainly located in the high latitude regions by comparing five different climate models. The potential reason is related to uncertainties of the freshwater forcing and the latitude of

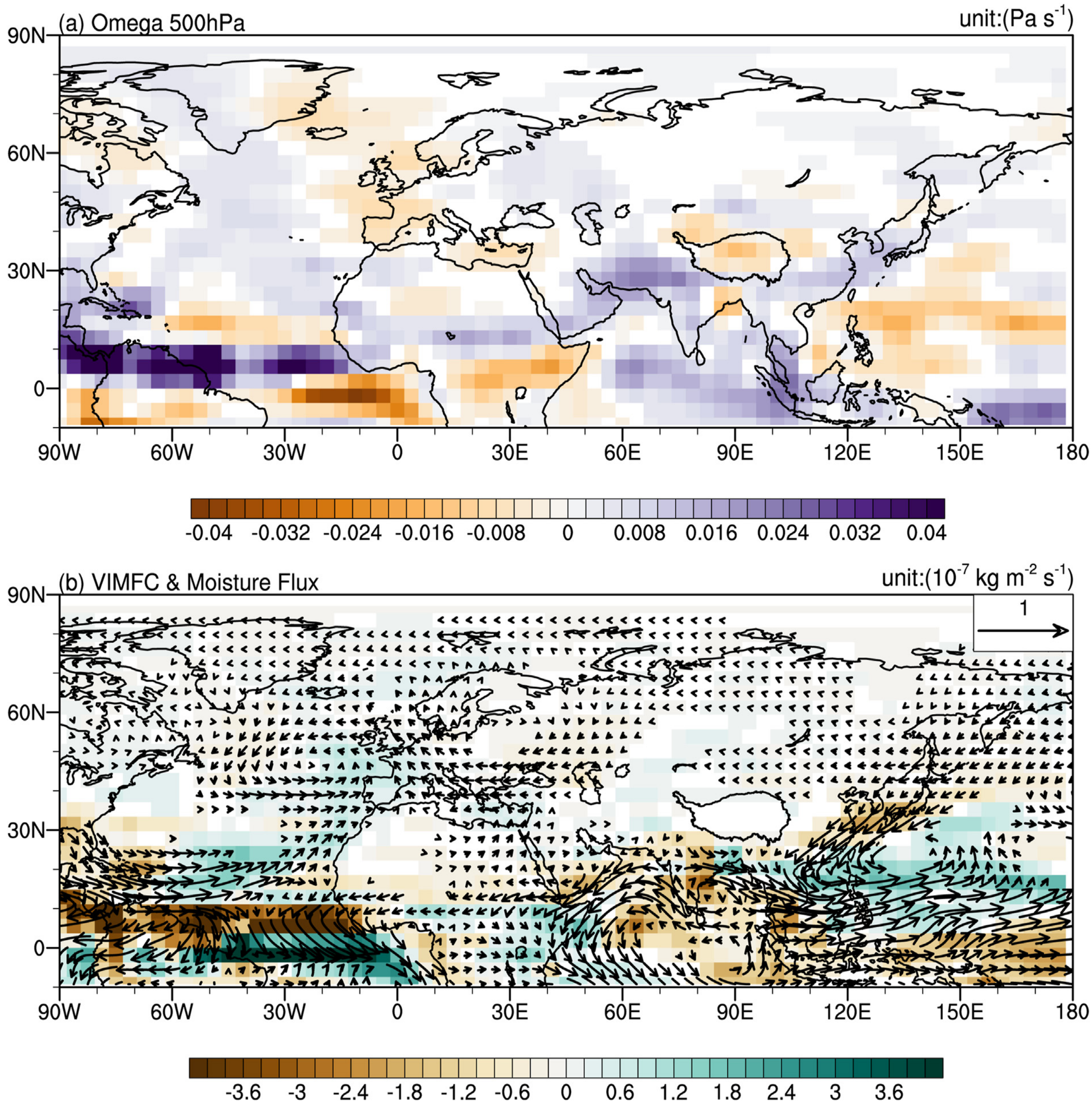

Fig. 10. Changes in vertical motion and moisture transport during summer in the TraCE-MWF simulation during the YD. (a) vertical motion at 500 hPa. Negative values represent an increase in upward motion, (b) integrated moisture flux (vectors) and moisture convergence (shaded). Negative values mean moisture divergence. Only differences that exceed the 95% significant level are plotted.

the strongest cooling depends on the location of the North Atlantic Deep Water. Although the relatively realistic forcing conditions are adopted in the TraCE data, it might still underestimate the cooling over Greenland and North Atlantic (He, 2011). Previous studies also indicated different sensitivity of the AMOC and that the responses of temperature over the northern North Atlantic varied greatly among models (Stouffer et al., 2006). Based on the modern water-hosing experiments, the strength of EASM shows different responses, which depends on the magnitude of the AMOC related to the freshwater discharge. Yu et al. (2018) figured out that a subtle weakening of AMOC did not result in the significant changes of EASM, and the effect on the EASM only took place when the AMOC weakened more substantially. On the other hand, there still exist some debates about the interpretation of the cave $\delta^{18}O$ in Asia although they are widely used as major proxies to investigate the summer monsoon variations in the past. Cave $\delta^{18}O$ may mostly present the large-scale monsoon intensity rather than the amount of local precipitation (Cheng et al., 2012; Clemens et al., 2010).

5. Conclusions

Using transient climate modeling data over the last 21,000 years, the climate responses, attributions, and potential mechanisms over Asia during the YD episode are investigated in this study. The results show that the whole Asia experiences cool and dry conditions and this response is mainly attributed to the melt-water flux and associated cooling over North Atlantic. Weakened East Asian and Indian summer monsoon are also found, which can be explained by a weaker surface land-sea thermal gradient and/or an eastward wave train pattern from the North Atlantic to Eurasia in the upper troposphere. Although the coarsely spatial resolution of these modeling data may limit the performance of the Asian climate simulation, our work provides useful insights into the spatial patterns and dynamics of the millennial-scale rapid Asian climate change, such as YD and Heinrich events. Future studies by higher resolution climate models are still necessary to fully assess how the Asian climate responds to various external forcings and especially the meltwater discharge.

Credit author statement

Jie Wu: Methodology, Formal analysis, Visualization, Writing – original draft. **Zhengguo Shi**: Conceptualization, Methodology, Supervision, Writing – review & editing. **Yongheng Yang**: Investigation, Visualization.

Declaration of competing interest

The authors declare that they have no known competing financial interests or personal relationships that could have appeared to influence the work reported in this paper.

Data availability

The TraCE-21ka data used in this study can be accessed through the website of Earth System Grid (https://www.earthsystemgrid.org/project/trace.html)

Acknowledgements

We appreciate two anonymous reviewers for their constructive comments and suggestions, which are of great help to improve our manuscript. This work is jointly supported by the Strategic Priority Research Program of Chinese Academy of Sciences (XDB40030000) and National Natural Science Foundation of China (41888101, 41977382). Z. Shi also acknowledges the support of the Youth Innovation Promotion Association of the Chinese Academy of Sciences and Natural Science basic Research Program of Shaanxi Province (2022JC-17). We thank the TraCE-21ka group for providing their model output via the Earth System Grid of the National Center for Atmospheric Research. The model data are available online (https://www.earthsystemgrid.org/project/trace.html).

References

Alley, R.B., 2007. Wally was right: predictive ability of the north atlantic "conveyor belt" hypothesis for abrupt climate change. Annu. Rev. Earth Planet Sci. 35, 241–272. https://doi.org/10.1146/annurev.earth.35.081006.131524.

Alley, R.B., 2000. The Younger Dryas cold interval as viewed from central Greenland. Quat. Sci. Rev. 19, 213–226. https://doi.org/10.1016/S0277-3791(99)00062-1.

Alley, R.B., Meese, D.A., Shuman, C.A., Gow, A.J., Taylor, K.C., Grootes, P.M., White, J.W.C., Ram, M., Waddington, E.D., Mayewski, P.A., Zielinski, G.A., 1993. Abrupt increase in Greenland snow accumulation at the end of the Younger Dryas event. Nature 362, 527–529. https://doi.org/10.1038/362527a0.

An, Z., Porter, S.C., Weijian, Z., Yanchou, L., Donahue, D.J., Head, M.J., Xihuo, W., Jianzhang, R., Hongbo, Z., 1993. Episode of strengthened summer monsoon climate of younger Dryas age on the loess plateau of Central China. Quat. Res. 39, 45–54. https://doi.org/10.1006/qres.1993.1005.

Beck, J.W., Zhou, W., Li, C., Wu, Z., White, L., Xian, F., Kong, X., An, Z., 2018. A 550,000-year record of East Asian monsoon rainfall from 10 Be in loess. Science 360, 877–881. https://doi.org/10.1126/science.aam5825.

Berger, A., 1978. Long-term variations of daily insolation and quaternary climatic changes. J. Atmos. Sci. 35, 2362–2367. https://doi.org/10.1175/1520-0469(1978)035<2362:LTVODI>2.0.CO;2.

Boyle, E.A., Keigwin, L., 1987. North Atlantic thermohaline circulation during the past 20,000 years linked to high-latitude surface temperature. Nature 330, 35–40. https://doi.org/10.1038/330035a0.

Brauer, A., Endres, C., Günter, C., Litt, T., Stebich, M., Negendank, J.F.W., 1999. High resolution sediment and vegetation responses to Younger Dryas climate change in varved lake sediments from Meerfelder Maar, Germany. Quat. Sci. Rev. 18, 321–329. https://doi.org/10.1016/S0277-3791(98)00084-5.

Broecker, W.S., Andree, M., Wolfli, W., Oeschger, H., Bonani, G., Kennett, J., Peteet, D., 1988. The chronology of the last deglaciation: implications to the cause of the younger Dryas event. Paleoceanography 3, 1–19. https://doi.org/10.1029/PA003i001p00001.

Broecker, W.S., Kennett, J.P., Flower, B.P., Teller, J.T., Trumbore, S., Bonani, G., Wolfli, W., 1989. Routing of meltwater from the Laurentide ice sheet during the younger Dryas cold episode. Nature 341, 318–321. https://doi.org/10.1038/341318a0.

Broecker, W.S., Peteet, D.M., Rind, D., 1985. Does the ocean–atmosphere system have more than one stable mode of operation? Nature 315, 21–26. https://doi.org/10.1038/315021a0.

Carlson, A.E., 2013. PALEOCLIMATE | the younger Dryas climate event. In: Encyclopedia of Quaternary Science. Elsevier, pp. 126–134. https://doi.org/10.1016/B978-0-444-53643-3.00029-7.

Chen, F., Xu, Q., Chen, J., Birks, H.J.B., Liu, J., Zhang, S., Jin, L., An, C., Telford, R.J., Cao, X., Wang, Z., Zhang, X., Selvaraj, K., Lu, H., Li, Y., Zheng, Z., Wang, H., Zhou, A., Dong, G., Zhang, J., Huang, X., Bloemendal, J., Rao, Z., 2015. East Asian summer monsoon precipitation variability since the last deglaciation. Sci. Rep. 5, 11186. https://doi.org/10.1038/srep11186.

Chen, X., Wu, D., Huang, X., Lv, F., Brenner, M., Jin, H., Chen, F., 2020. Vegetation response in subtropical southwest China to rapid climate change during the Younger Dryas. Earth Sci. Rev. 201, 103080. https://doi.org/10.1016/j.earscirev.2020.103080.

Cheng, H., Sinha, A., Wang, X., Cruz, F.W., Edwards, R.L., 2012. The global paleomonsoon as seen through speleothem records from Asia and the americas. Clim. Dynam. 39, 1045–1062. https://doi.org/10.1007/s00382-012-1363-7.

Cheng, H., Zhang, H., Spötl, C., Baker, J., Sinha, A., Li, H., , Bartolomé, M., Moreno, A., Kathayat, G., Zhao, J., Dong, X., Li, Y., Ning, Y., Jia, X., Zong, B., Ait Brahim, Y., Pérez-Mejías, C., Cai, Y., Novello, V.F., Cruz, F.W., Severinghaus, J.P., An, Z., Edwards, R.L., 2020. Timing and structure of the Younger Dryas event and its underlying climate dynamics. Proc. Natl. Acad. Sci. USA 117, 23408–23417. https://doi.org/10.1073/pnas.2007869117.

Clemens, S.C., Prell, W.L., Sun, Y., 2010. Orbital-scale timing and mechanisms driving Late Pleistocene Indo-Asian summer monsoons: reinterpreting cave speleothem $\delta^{18}O$. Paleoceanography 25, PA4207. https://doi.org/10.1029/2010PA001926.

Clement, A.C., Cane, M.A., Seager, R., 2001. An orbitally driven tropical source for abrupt climate change. J. Clim. 14, 2369–2375. https://doi.org/10.1175/1520-0442(2001)014<2369:AODTSF>2.0.CO;2.

Collins, W.D., Bitz, C.M., Blackmon, M.L., Bonan, G.B., Bretherton, C.S., Carton, J.A., Chang, P., Doney, S.C., Hack, J.J., Henderson, T.B., Kiehl, J.T., Large, W.G., McKenna, D.S., Santer, B.D., Smith, R.D., 2006. The community climate system model version 3 (CCSM3). J. Clim. 19, 2122–2143. https://doi.org/10.1175/JCLI3761.1.

Dahl, K.A., Broccoli, A.J., Stouffer, R.J., 2005. Assessing the role of North Atlantic freshwater forcing in millennial scale climate variability: a tropical Atlantic perspective. Clim. Dynam. 24, 325–346. https://doi.org/10.1007/s00382-004-0499-5.

Dansgaard, W., White, J.W.C., Johnsen, S.J., 1989. The abrupt termination of the Younger Dryas climate event. Nature 339, 532–534. https://doi.org/10.1038/339532a0.

deMenocal, P., Ortiz, J., Guilderson, T., Sarnthein, M., 2000. Coherent high- and low-latitude climate variability during the Holocene warm period. Science 288, 2198–2202. https://doi.org/10.1126/science.288.5474.2198.

Ding, X., Bao, H., Zheng, L., Li, D., Kao, S.-J., 2017. Lacustrine lignin biomarker record reveals a severe drought during the late Younger Dryas in southern Taiwan. J. Asian Earth Sci. 135, 281–290. https://doi.org/10.1016/j.jseaes.2017.01.003.

Dong, B.-W., Sutton, R.T., 2002. Adjustment of the coupled ocean-atmosphere system to a sudden change in the Thermohaline Circulation. Geophys. Res. Lett. 29, 18-1–18–4. https://doi.org/10.1029/2002GL015229.

Dorale, J.A., Wozniak, L.A., Bettis, E.A., Carpenter, S.J., Mandel, R.D., Hajic, E.R., Lopinot, N.H., Ray, J.H., 2010. Isotopic evidence for younger Dryas aridity in the north American midcontinent. Geology 38, 519–522. https://doi.org/10.1130/G30781.1.

Dykoski, C., Edwards, R., Cheng, H., Yuan, D., Cai, Y., Zhang, M., Lin, Y., Qing, J., An, Z., Revenaugh, J., 2005. A high-resolution, absolute-dated Holocene and deglacial Asian monsoon record from Dongge Cave, China. Earth Planet Sci. Lett. 233, 71–86. https://doi.org/10.1016/j.epsl.2005.01.036.

Firestone, R.B., West, A., Kennett, J.P., Becker, L., Bunch, T.E., Revay, Z.S., Schultz, P.H., Belgya, T., Kennett, D.J., Erlandson, J.M., Dickenson, O.J., Goodyear, A.C., Harris, R.S., Howard, G.A., Kloosterman, J.B., Lechler, P., Mayewski, P.A., Montgomery, J., Poreda, R., Darrah, T., Hee, S.S.Q., Smith, A.R., Stich, A., Topping, W., Wittke, J.H., Wolbach, W.S., 2007. Evidence for an extraterrestrial impact 12,900 years ago that contributed to the megafaunal extinctions and the Younger Dryas cooling. Proc. Natl. Acad. Sci. USA 104, 16016–16021. https://doi.org/10.1073/pnas.0706977104.

Fukusawa, H., 1999. Varved lacustrine sediments in Japan: recent progress. Quat. Res. 38, 237–243. https://doi.org/10.4116/jaqua.38.237.

Gasse, F., Van Campo, E., 1994. Abrupt post-glacial climate events in West Asia and North Africa monsoon domains. Earth Planet Sci. Lett. 126, 435–456. https://doi.org/10.1016/0012-821X(94)90123-6.

Genty, D., Blamart, D., Ghaleb, B., Plagnes, V., Causse, C., Bakalowicz, M., Zouari, K., Chkir, N., Hellstrom, J., Wainer, K., 2006. Timing and dynamics of the last

deglaciation from European and North African δ13C stalagmite profiles—comparison with Chinese and South Hemisphere stalagmites. Quat. Sci. Rev. 25, 2118–2142. https://doi.org/10.1016/j.quascirev.2006.01.030.
Grafenstein, U. von, Erlenkeuser, H., Brauer, A., Jouzel, J., Johnsen, S.J., 1999. A mid-European decadal isotope-climate record from 15,500 to 5000 Years B.P. Science 284, 1654–1657. https://doi.org/10.1126/science.284.5420.1654.
Hajdas, I., Bonani, G., Moreno, P.I., Ariztegui, D., 2003. Precise radiocarbon dating of Late-Glacial cooling in mid-latitude South America. Quat. Res. 59, 70–78. https://doi.org/10.1016/S0033-5894(02)00017-0.
He, F., 2011. Simulating Transient Climate Evolution of the Last Deglaciation with CCSM3. Ph D. thesis. University of Wisconsin-Madison, p. 171. http://www.cgd.ucar.edu/ccr/TraCE/doc/He_PhD_dissertation_UW_2011.pdf.
He, F., Shakun, J.D., Clark, P.U., Carlson, A.E., Liu, Z., Otto-Bliesner, B.L., Kutzbach, J.E., 2013. Northern Hemisphere forcing of Southern Hemisphere climate during the last deglaciation. Nature 494, 81–85. https://doi.org/10.1038/nature11822.
Herzschuh, U., 2006. Palaeo-moisture evolution in monsoonal Central Asia during the last 50,000 years. Quat. Sci. Rev. 25, 163–178. https://doi.org/10.1016/j.quascirev.2005.02.006.
Johnsen, S.J., Clausen, H.B., Dansgaard, W., Fuhrer, K., Gundestrup, N., Hammer, C.U., Iversen, P., Jouzel, J., Stauffer, B., Steffensen, J.P., 1992. Irregular glacial interstadials recorded in a new Greenland ice core. Nature 359, 311–313. https://doi.org/10.1038/359311a0.
Johnson, R.G., McClure, B.T., 1976. A model for northern hemisphere continental ice sheet variation. Quat. Res. 6, 325–353. https://doi.org/10.1016/0033-5894(67)90001-4.
Joos, F., Spahni, R., 2008. Rates of change in natural and anthropogenic radiative forcing over the past 20,000 years. Proc. Natl. Acad. Sci. USA 105, 1425–1430. https://doi.org/10.1073/pnas.0707386105.
Keigwin, L.D., Jones, G.A., 1990. Deglacial climatic oscillations in the Gulf of California. Paleoceanography 5, 1009–1023. https://doi.org/10.1029/PA005i006p01009.
Kubota, Y., Kimoto, K., Tada, R., Oda, H., Yokoyama, Y., Matsuzaki, H., 2010. Variations of East Asian summer monsoon since the last deglaciation based on Mg/Ca and oxygen isotope of planktic foraminifera in the northern East China Sea. Paleoceanography 25, PA4205. https://doi.org/10.1029/2009PA001891.
Kudrass, H.R., Erlenkeuser, H., Vollbrecht, R., Weiss, W., 1991. Global nature of the Younger Dryas cooling event inferred from oxygen isotope data from Sulu Sea cores. Nature 349, 406–409. https://doi.org/10.1038/349406a0.
Liu, D., Wang, Y., Cheng, H., Edwards, R.L., Kong, X., Wang, X., Wu, J., Chen, S., 2008. A detailed comparison of Asian Monsoon intensity and Greenland temperature during the Allerød and Younger Dryas events. Earth Planet Sci. Lett. 272, 691–697. https://doi.org/10.1016/j.epsl.2008.06.008.
Liu, Z., Carlson, A.E., He, F., Brady, E.C., Otto-Bliesner, B.L., Briegleb, B.P., Wehrenberg, M., Clark, P.U., Wu, S., Cheng, J., Zhang, J., Noone, D., Zhu, J., 2012. Younger Dryas cooling and the Greenland climate response to CO2. Proc. Natl. Acad. Sci. USA 109, 11101–11104. https://doi.org/10.1073/pnas.1202183109.
Lu, R., Dong, B., 2008. Response of the Asian summer monsoon to weakening of Atlantic thermohaline circulation. Adv. Atmos. Sci. 25, 723–736. https://doi.org/10.1007/s00376-008-0723-z.
Ma, Z.-B., Cheng, H., Tan, M., Edwards, R.L., Li, H.-C., You, C.-F., Duan, W.-H., Wang, X., Kelly, M.J., 2012. Timing and structure of the Younger Dryas event in northern China. Quat. Sci. Rev. 41, 83–93. https://doi.org/10.1016/j.quascirev.2012.03.006.
Manabe, S., Stouffer, R.J., 1997. Coupled ocean-atmosphere model response to freshwater input: comparison to Younger Dryas Event. Paleoceanography 12, 321–336. https://doi.org/10.1029/96PA03932.
Manabe, S., Stouffer, R.J., 1988. Two stable equilibria of a coupled ocean-atmosphere model. J. Clim. 1, 841–866. https://doi.org/10.1175/1520-0442(1988)001<0841:TSEOAC>2.0.CO;2.
Marzin, Charline, Braconnot, P., Kageyama, M., 2013. Relative impacts of insolation changes, meltwater fluxes and ice sheets on African and Asian monsoons during the Holocene. Clim. Dynam. 41, 2267–2286. https://doi.org/10.1007/s00382-013-1948-9.
McManus, J.F., Francois, R., Gherardi, J.-M., Keigwin, L.D., Brown-Leger, S., 2004. Collapse and rapid resumption of Atlantic meridional circulation linked to deglacial climate changes. Nature 428, 834–837. https://doi.org/10.1038/nature02494.
Moreno, P.I., Kaplan, M.R., François, J.P., Villa-Martínez, R., Moy, C.M., Stern, C.R., Kubik, P.W., 2009. Renewed glacial activity during the Antarctic cold reversal and persistence of cold conditions until 11.5 ka in southwestern Patagonia. Geology 37, 375–378. https://doi.org/10.1130/G25399A.1.
Morley, D.W., Leng, M.J., Mackay, A.W., Sloane, H.J., 2005. Late glacial and Holocene environmental change in the Lake Baikal region documented by oxygen isotopes from diatom silica. Global Planet. Change 46, 221–233. https://doi.org/10.1016/j.gloplacha.2004.09.018.
Murton, J.B., Bateman, M.D., Dallimore, S.R., Teller, J.T., Yang, Z., 2010. Identification of younger Dryas outburst flood path from Lake Agassiz to the Arctic Ocean. Nature 464, 740–743. https://doi.org/10.1038/nature08954.
Nakagawa, T., Kitagawa, H., Yasuda, Y., Tarasov, P.E., Nishida, K., Gotanda, K., Sawai, Y., 2003. Asynchronous climate changes in the north atlantic and Japan during the last termination. Science 299, 688–691. https://doi.org/10.1126/science.1078235.
Nakagawa, T., Tarasov, P.E., Kitagawa, H., Yasuda, Y., Gotanda, K., 2006. Seasonally specific responses of the East Asian monsoon to deglacial climate changes. Geology 34, 521. https://doi.org/10.1130/G21764.1.
Okumura, Y.M., Deser, C., Hu, A., Timmermann, A., Xie, S.-P., 2009. North pacific climate response to freshwater forcing in the subarctic North Atlantic: oceanic and atmospheric pathways. J. Clim. 22, 1424–1445. https://doi.org/10.1175/2008JCLI2511.1.
Park, J., Lim, H.S., Lim, J., Park, Y.-H., 2014. High-resolution multi-proxy evidence for millennial- and centennial-scale climate oscillations during the last deglaciation in Jeju Island, South Korea. Quat. Sci. Rev. 105, 112–125. https://doi.org/10.1016/j.quascirev.2014.10.003.
Peltier, W.R., 2004. Global glacial isostasy and the surface of the ice-age earth: the ICE-5G (VM2) model and grace. Annu. Rev. Earth Planet Sci. 32, 111–149. https://doi.org/10.1146/annurev.earth.32.082503.144359.
Pinter, N., Scott, A.C., Daulton, T.L., Podoll, A., Koeberl, C., Anderson, R.S., Ishman, S.E., 2011. The Younger Dryas impact hypothesis: a requiem. Earth Sci. Rev. 106, 247–264. https://doi.org/10.1016/j.earscirev.2011.02.005.
Rashid, H., Flower, B.P., Poore, R.Z., Quinn, T.M., 2007. A ~25ka Indian Ocean monsoon variability record from the Andaman Sea. Quat. Sci. Rev. 26, 2586–2597. https://doi.org/10.1016/j.quascirev.2007.07.002.
Rasmussen, S.O., Andersen, K.K., Svensson, A.M., Steffensen, J.P., Vinther, B.M., Clausen, H.B., Siggaard-Andersen, M.-L., Johnsen, S.J., Larsen, L.B., Dahl-Jensen, D., Bigler, M., Röthlisberger, R., Fischer, H., Goto-Azuma, K., Hansson, M.E., Ruth, U., 2006. A new Greenland ice core chronology for the last glacial termination. J. Geophys. Res. 111, D06102. https://doi.org/10.1029/2005JD006079.
Renssen, H., 2020. Comparison of climate model simulations of the younger Dryas cold event. Quaternary 3, 29. https://doi.org/10.3390/quat3040029.
Renssen, H., Geel, B. Van, Plicht, J. Van Der, Magny, M., 2000. Reduced solar activity as a trigger for the start of the Younger Dryas? Quat. Int. 68–71, 373–383. https://doi.org/10.1016/S1040-6182(00)00060-4.
Renssen, H., Mairesse, A., Goosse, H., Mathiot, P., Heiri, O., Roche, D.M., Nisancioglu, K.H., Valdes, P.J., 2015. Multiple causes of the Younger Dryas cold period. Nat. Geosci. 8, 946–949. https://doi.org/10.1038/ngeo2557.
Rooth, C., 1982. Hydrology and ocean circulation. Prog. Oceanogr. 11, 131–149. https://doi.org/10.1016/0079-6611(82)90006-4.
Shakun, J.D., Burns, S.J., Fleitmann, D., Kramers, J., Matter, A., Al-Subary, A., 2007. A high-resolution, absolute-dated deglacial speleothem record of Indian Ocean climate from Socotra Island, Yemen. Earth Planet Sci. Lett. 259, 442–456. https://doi.org/10.1016/j.epsl.2007.05.004.
Shi, J., Yan, Q., 2019. Evolution of the asian–african monsoonal precipitation over the last 21 kyr and the associated dynamic mechanisms. J. Clim. 32, 6551–6569. https://doi.org/10.1175/JCLI-D-19-0074.1.
Shuman, B., Bartlein, P.J., Webb, T., 2005. The magnitudes of millennial- and orbital-scale climatic change in eastern North America during the Late Quaternary. Quat. Sci. Rev. 24, 2194–2206. https://doi.org/10.1016/j.quascirev.2005.03.018.
Sinha, A., Cannariato, K.G., Stott, L.D., Li, H.-C., You, C.-F., Cheng, H., Edwards, R.L., Singh, I.B., 2005. Variability of Southwest Indian summer monsoon precipitation during the Bølling-Ållerød. Geology 33, 813–816. https://doi.org/10.1130/G21498.1.
Steffensen, J.P., Andersen, K.K., Bigler, M., Clausen, H.B., Dahl-Jensen, D., Fischer, H., Goto-Azuma, K., Hansson, M., Johnsen, S.J., Jouzel, J., Masson-Delmotte, V., Popp, T., Rasmussen, S.O., Röthlisberger, R., Ruth, U., Stauffer, B., Siggaard-Andersen, M.-L., Sveinbjörnsdóttir, A.E., Svensson, A., White, J.W.C., 2008. High-resolution Greenland ice core data show abrupt climate change happens in few years. Science 321, 680–684. https://doi.org/10.1126/science.1157707.
Stouffer, R.J., Yin, J., Gregory, J.M., Dixon, K.W., Spelman, M.J., Hurlin, W., Weaver, A.J., Eby, M., Flato, G.M., Hasumi, H., Hu, A., Jungclaus, J.H., Kamenkovich, I.V., Levermann, A., Montoya, M., Murakami, S., Nawrath, S., Oka, A., Peltier, W.R., Robitaille, D.Y., Sokolov, A., Vettoretti, G., Weber, S.L., 2006. Investigating the causes of the response of the thermohaline circulation to past and future climate changes. J. Clim. 19, 1365–1387. https://doi.org/10.1175/JCLI3689.1.
Sun, Y., Clemens, S.C., Morrill, C., Lin, X., Wang, X., An, Z., 2012. Influence of Atlantic meridional overturning circulation on the East Asian winter monsoon. Nat. Geosci. 5, 46–49. https://doi.org/10.1038/ngeo1326.
Sun, Y., Oppo, D.W., Xiang, R., Liu, W., Gao, S., 2005. Last deglaciation in the okinawa trough: subtropical northwest pacific link to northern hemisphere and tropical climate. Paleoceanography 20, PA4005. https://doi.org/10.1029/2004PA001061.
Sundaram, S., Yin, Q.Z., Berger, A., Muri, H., 2012. Impact of ice sheet induced North Atlantic oscillation on East Asian summer monsoon during an interglacial 500,000 years ago. Clim. Dynam. 39, 1093–1105. https://doi.org/10.1007/s00382-011-1213-z.
Takahara, H., Igarashi, Y., Hayashi, R., Kumon, F., Liew, P.-M., Yamamoto, M., Kawai, S., Oba, T., Irino, T., 2010. Millennial-scale variability in vegetation records from the east asian islands: taiwan, Japan and sakhalin. Quat. Sci. Rev. 29, 2900–2917. https://doi.org/10.1016/j.quascirev.2009.11.026.
Timmermann, A., Okumura, Y., An, S.I., Clement, A., Dong, B., Guilyardi, E., Hu, A., Jungclaus, J.H., Renold, M., Stocker, T.F., Stouffer, R.J., Sutton, R., Xie, S.P., Yin, J., 2007. The influence of a weakening of the Atlantic meridional overturning circulation on ENSO. J. Clim. 20, 4899–4919. https://doi.org/10.1175/JCLI4283.1.
Vellinga, M., Wood, R.A., 2002. Global climatic impacts of a collapse of the atlantic thermohaline circulation. In: Climatic Change. Springer Netherlands, Dordrecht, pp. 251–267. https://doi.org/10.1023/A:1016168827653.
Wang, Y.J., Cheng, H., Edwards, R.L., An, Z.S., Wu, J.Y., Shen, C.C., Dorale, J.A., 2001. A high-resolution absolute-dated late pleistocene monsoon record from Hulu Cave, China. Science 294, 2345–2348. https://doi.org/10.1126/science.1064618.
Wen, X., Liu, Z., Wang, S., Cheng, J., Zhu, J., 2016. Correlation and anti-correlation of the East Asian summer and winter monsoons during the last 21,000 years. Nat.

Commun. 7, 11999. https://doi.org/10.1038/ncomms11999.
Wu, L., Li, C., Yang, C., Xie, S.-P., 2008. Global teleconnections in response to a shutdown of the atlantic meridional overturning circulation. J. Clim. 21, 3002–3019. https://doi.org/10.1175/2007JCLI1858.1.
Wu, Z., Wang, B., Li, J., Jin, F.-F., 2009. An empirical seasonal prediction model of the east Asian summer monsoon using ENSO and NAO. J. Geophys. Res. 114, D18120. https://doi.org/10.1029/2009JD011733.
Wunsch, C., 2006. Abrupt climate change: an alternative view. Quat. Res. 65, 191–203. https://doi.org/10.1016/j.yqres.2005.10.006.
Yeager, S.G., Shields, C.A., Large, W.G., Hack, J.J., 2005. The low-resolution CCSM3. J. Clim. 19, 2545–2566. https://doi.org/10.1175/JCLI3744.1.
Yu, L., Gao, Y., Wang, H., Guo, D., Li, S., 2009. The responses of East asian summer monsoon to the north atlantic meridional overturning circulation in an enhanced freshwater input simulation. Sci. Bull. 54, 4724–4732. https://doi.org/10.1007/s11434-009-0720-3.
Yu, T., Cheng, J., Lin, P., Yu, Y., Guo, P., 2018. Responses and mechanisms of East Asian winter and summer monsoons to weakened Atlantic meridional overturning circulation using the FGOALS-g2 model. Int. J. Climatol. 38, 2618–2626. https://doi.org/10.1002/joc.5373.
Yuan, D., Cheng, H., Edwards, R.L., Dykoski, C.A., Kelly, M.J., Zhang, M., Qing, J., Lin, Y., Wang, Y., Wu, J., Dorale, J.A., An, Z., Cai, Y., 2004. Timing, duration, and transitions of the last interglacial asian monsoon. Science 304, 575–578. https://doi.org/10.1126/science.1091220.
Zhang, R., Delworth, T.L., 2005. Simulated tropical response to a substantial weakening of the atlantic thermohaline circulation. J. Clim. 18, 1853–1860. https://doi.org/10.1175/JCLI3460.1.
Zheng, F., Li, J., Li, Y., Zhao, S., Deng, D., 2016. Influence of the summer NAO on the spring-NAO-based predictability of the east asian summer monsoon. J. Appl. Meteorol. Climatol. 55, 1459–1476. https://doi.org/10.1175/JAMC-D-15-0199.1.
Zhou, W., Head, M., Lu, X., An, Z., Jull, A.J., Donahue, D., 1999. Teleconnection of climatic events between East Asia and polar, high latitude areas during the last deglaciation. Palaeogeogr. Palaeoclimatol. Palaeoecol. 152, 163–172. https://doi.org/10.1016/S0031-0182(99)00041-3.
Zhou, W., Xian, F., Du, Y., Kong, X., Wu, Z., 2014. The last 130 ka precipitation reconstruction from Chinese loess 10 Be. J. Geophys. Res. Solid Earth 119, 191–197. https://doi.org/10.1002/2013JB010296.
Zuo, J., Li, W., Sun, C., Xu, L., Ren, H.-L., 2013. Impact of the North Atlantic sea surface temperature tripole on the East Asian summer monsoon. Adv. Atmos. Sci. 30, 1173–1186. https://doi.org/10.1007/s00376-012-2125-5.